Comparative study of density analysis using automated whole breast ultrasound and MRI

Woo Kyung Moon
Department of Radiology, Seoul National University Hospital, Seoul 110–744, Korea

Yi-Wei Shen
Department of Computer Science and Information Engineering, National Taiwan University, Taipei 10617, Taiwan

Chiun-Sheng Huang
Department of Surgery, National Taiwan University Hospital, Taipei 100, Taiwan

Sheng-Chy Luo
Department of Computer Science and Information Engineering, National Taiwan University, Taipei 10617, Taiwan

Aida Kuzucan
Department of Radiological Science and Center for Functional Onco-Imaging, University of California Irvine, Irvine, California 92697

Jeon-Hor Chen[a),b)]
Department of Radiological Science and Center for Functional Onco-Imaging, University of California Irvine, Irvine, California 92697 and Department of Radiology, China Medical University Hospital, Taichung 40402, Taiwan

Ruey-Feng Chang[a),c)]
Department of Computer Science and Information Engineering, National Taiwan University, Taipei 10617, Taiwan and Graduate Institute of Biomedical Electronics and Bioinformatics, National Taiwan University, Taipei 10617, Taiwan

(Received 25 May 2010; revised 27 October 2010; accepted for publication 12 November 2010; published 22 December 2010)

Purpose: The purpose of this study is to compare the measurements of breast density using three-dimensional (3-D) automated whole breast ultrasound (ABUS) and magnetic resonance imaging (MRI).
Methods: In this study, 3-D ABUS and MRI breast images were obtained from 40 patients—bilaterally in 27 patients and unilaterally (due to operation in the contralateral breast) in 13 patients. To differentiate the fibroglandular and fatty tissues in ABUS and MRI images, the fuzzy C-mean classifier was used. Calculated values for percent density and breast volume from the two modalities were compared to and correlated with linear regression analysis. Intraoperator and interoperator variations among eight cases were evaluated to verify the consistency of the density analysis.
Results: Mean percent density and breast volume derived from ABUS ($17.63 \pm 11.87\%$ and 418.30 ± 132.97 cm^3, respectively) and MRI images ($23.79 \pm 16.62\%$ and 544.90 ± 207.41 cm^3) demonstrated good correlation ($R=0.917$ and $R=0.884$). Intraoperator and interoperator analyses yielded slightly larger coefficients of variation for percent density and breast volume in ABUS compared to MRI. However, the differences were not statistically significant.
Conclusions: ABUS and MRI showed high correlation for breast density and breast volume quantification. Both modalities could provide useful breast density information to physicians. © *2011 American Association of Physicists in Medicine*. [DOI: 10.1118/1.3523617]

Key words: automated breast ultrasound, MRI, breast density, fuzzy C-mean

I. INTRODUCTION

Breast density, a relative value for the amount of fibroglandular tissue (stromal and epithelial) in the breast, can be affected by various genetic, hormonal, and environmental factors.[1–6] Mammographically determined dense breasts in women have been correlated with a breast cancer risk 1.8–6.0 times that of women with lower densities.[2,7–9] Despite common clinical use, evaluations of breast density based on mammograms suffer from major problems including tissue overlap, inconsistent values due to variation in the position and degree of compression, and variation in the calibration.[10,11] Recently, efforts toward developing more reliable imaging techniques for assessing breast density for cancer risk correlation have turned to magnetic resonance imaging (MRI) as a possible modality.[12–22] MRI provides a three-dimensional (3-D) view of the breast, contrasting fib-

roglandular and fatty tissues without experiencing tissue overlap or x-ray exposure calibration. Unfortunately, consistent breast boundary parameters, pulse sequences, and computerized algorithms necessary to accurately segment fibroglandular tissue have not yet been established.

Several standardized automated breast ultrasound (ABUS) machines have been developed to acquire the volume of the whole breast.[23,24] In the study by Kelly *et al.*,[23] using ABUS with mammography, cancer detection was increased from 23 to 46 in 6425 examinations, compared to mammography alone. Previously, we analyzed breast density with ABUS images obtained from an Aloka SSD-5500 machine (Tokyo, Japan) with a probe width of 6 cm scanned in prone position.[22] The experimental results showed that the ABUS images could provide concordant and reliable quantification of breast density with the mammograms categorized based on ACR-BIRADS. In the current study, we aim to compare the results of breast density measurements between ABUS and MRI utilizing the fuzzy C-mean (FCM) method[18,21] to differentiate fibroglandular and fatty tissues.

II. MATERIALS AND METHODS

II.A. Patients

Between October 2007 and March 2008, imaging data were obtained from 40 patients of diagnostic setting (mean of age: 50.9; standard deviation of age: 9.4), with available ABUS and 3-D breast MRI images (mean time interval: 3.8 days; range, −70~73 days). Among the 40 patients, five patients had breast surgical operations and eight patients had abnormal findings in one breast. For these 13 patients, only 1 normal breast in each subject was analyzed. The remaining 27 patients had their bilateral breasts analyzed. In total, 67 breasts (bilateral breasts in 27 patients and 1 breast in 13 patients) were analyzed with two imaging modalities. Difference of breast density and breast volume of the two breasts for the same subject were analyzed in 27 patients. This study was approved by the local ethics committee and the informed consent was waived for our retrospective study.

II.B. The automated whole breast ultrasound

ABUS images were produced at a SomoVu ScanStation (U-systems, San Jose, CA). At the SomoVu ScanStation, the 10 MHz linear transducer with a width of 14.7 cm was used to obtain a wider US image compared to the conventional transducer with width of 4 cm.

Images were constructed of 2-D slices (548 ×348 pixels) from three orthogonal views, transverse (A view), longitudinal (B view), and coronal (C view), with a resolution of scanning of approximately 16 pixels/cm in the transverse direction (z-axis), 35 pixels/cm in the longitudinal direction (x-axis), and 88 pixels/cm in the coronal direction (y-axis). Skin, subcutaneous fat, glandular tissue, nipple, retromammary fat, muscle fascia, and ribs are observed in an A view shown in Fig. 1.

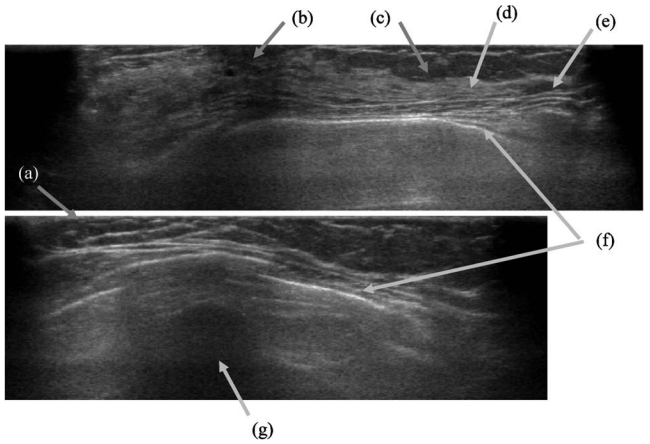

FIG. 1. The ABUS image in A view. (a) Skin, (b) nipple, (c) subcutaneous fat, (d) glandular tissues, (e) retromammary fat, (f) pectoral major muscle and pectoral minor muscle, and (g) rib.

II.C. Calculating percent density from ABUS images

The percent breast density was calculated based on the ratio of the fibroglandular tissue area over the whole breast regions, which together encompass breast tissue. Nonbreast regions—muscle, ribs, regions of overlap, skin, and anechoic regions—were removed prior to formulating percentage density values.

Muscle, ribs, and overlapping regions were removed manually. Regions of overlap between multiple images of the same breast were determined by creating a vertical line across the nipple as reference (Fig. 2). The nonbreast region below the retromammary fat was not included in the density analysis. The lowest horizontal plane in the C view that does not contain a muscle layer was selected manually to isolate muscle tissue. Isolation of the nonbreast region is demonstrated in Fig. 3. An improperly selected cutting line could result in the exclusion of breast tissue and the inclusion of muscle, which could affect density analysis. In ABUS im-

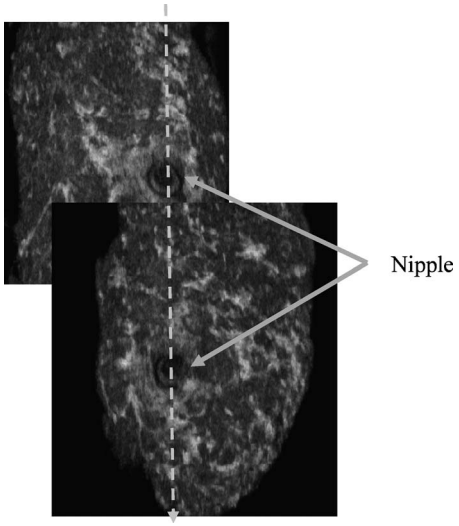

FIG. 2. Cutting the overlapping region at the nipple manually.

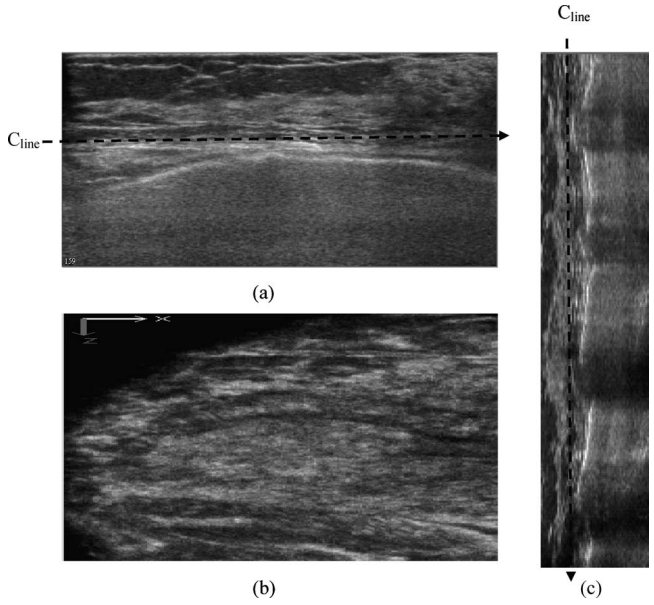

FIG. 3. Manually cutting the nonbreast region below the retromammary fat. (a) A view. (b) C view. (c) B view. In this case, the cutting line C_{line} is adopted to cut the nonbreast region below the retromammary fat.

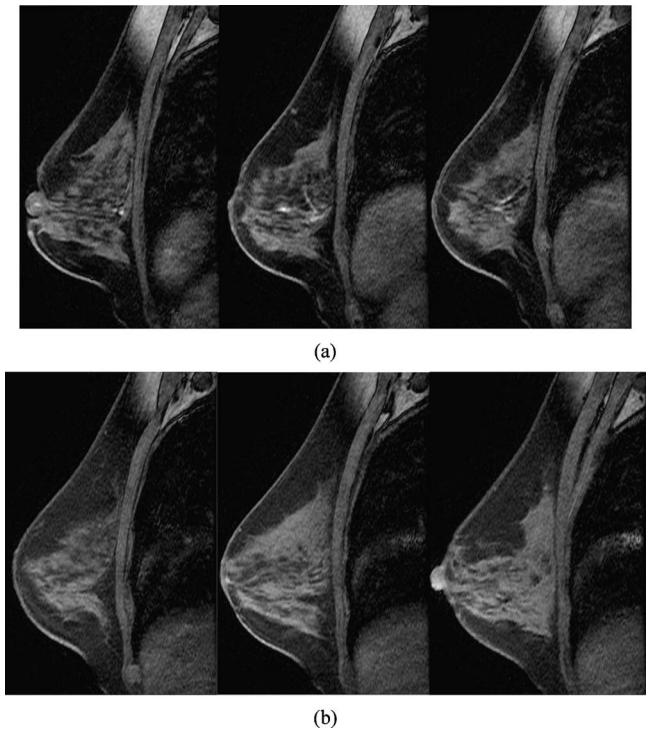

FIG. 4. A MRI image of the case in Fig. 1. (a) The sagittal slices 26, 33, and 36 of 3-D MRI image of right breast. (b) The sagittal slices 116, 122, and 130 of 3-D MRI image of left breast.

ages, high concentrations of speckle noise[25] can affect the result of a FCM classifier during density analysis. The anisotropic filter[25] was used to reduce this noise.

Skin and anechoic regions are removed individually by deleting the outmost 15 pixels (0.114 mm for a pixel; in total, 1.71 mm). In the anechoic regions, the probe does not have contact with the skin and no ultrasound signals exist. Mean values to remove anechoic regions of each vertical line were calculated from the outside to the inside in an A view slice. When the mean value was less than the anechoic threshold, $T_{ABUS\text{-}ac}$ was 20 in this experiment, the chosen vertical line was regarded as part of the anechoic region and the next inside vertical line marked the beginning of the breast region. Otherwise, the original vertical line and the remaining inside region were regarded as breast regions.

After isolation of the breast region, ABUS percent density was calculated with the following equation:

$$\text{percent density}_{ABUS} = \frac{\text{fibroglandular volume}_{ABUS}}{\text{total breast volume}_{ABUS}}, \quad (1)$$

where the fibroglandular volume_{ABUS} is the volume of fibroglandular tissue and the total breast volume_{ABUS} includes the volumes of fibroglandular tissue and fat.

II.D. Magnetic resonance imaging

MRI was performed with the GE Signa HDx 1.5 T (GE Medical Systems, Milwaukee, WI). The precontrast sagittal T1-weighted images with fat saturation were acquired using a 3-D VIBRANT (volume imaging for breast assessment) pulse sequence with TR=6.1 ms, TE=2.5 ms, image size =512×512, FOV=19 cm, and slice thickness=1.5 mm. The number of sagittal slices required to cover the entire breast were between 144 and 192. Some sagittal slices are shown in Fig. 4. The 3-D transverse MR images reconstructed from the acquired sagittal slices were used for the analysis of breast density.

The separation of the breast and chest was done by using the nipple and pectoralis muscle as reference. After determining the nipple position of the segmented breast in the transverse view, shown in Fig. 5(a), the coronal slices were scanned from the nipple to the chest until the two breasts were unified, shown in Fig. 5(b). The arrow indicates the minimum connecting region of the two breasts separating them. The lateral boundary of the breast was determined in the coronal slice and propagated to all other slices. The bounding box in Fig. 5(c) indicates the segmented region of the breast in the transverse view. The transverse bounding box in view was determined included the breast nipple and excluded the pectoralis muscle [Fig. 5(c)]. After separating the breast and chest, the skin line was segmented from the breast region. A lot of background noise and some blurred skin pixels made it difficult to extract the skin line using the simple thresholding technique. Hence, the detection method for skin pixels was proposed and used to check the pixels from left to right in the sagittal plane. In order to separate the breast and background regions, each pixel was checked whether it is due to breast tissue or the background noise from left to right in the sagittal plane. If the mean value was less than threshold, 100 in this experiment, the pixel was assumed to be due to background noise and the pixel checking continued from the current pixel to the right. Otherwise, the pixel checking finished and the right region of the pixel was considered breast tissue. In the FCM density analysis,

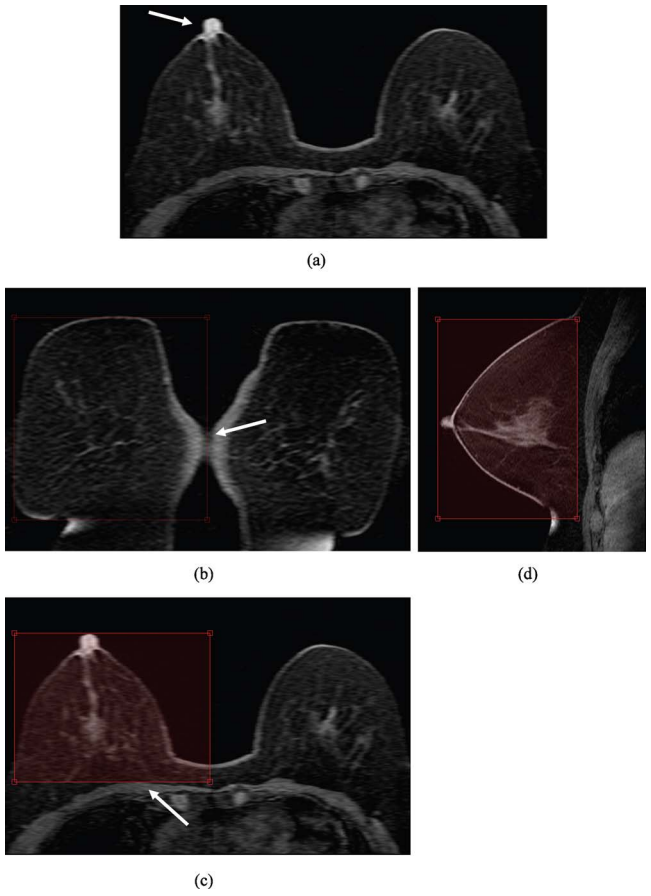

FIG. 5. The bounding box in three views for the MRI breast region. (a) The nipple is indicated by the arrow in the transverse view. (b) The lateral boundary of the breast is determined by the bounding box in the coronal view. The arrow indicates the minimum connected region of the two breasts which could separate the two breasts. (c) The segmented breast is determined by the bounding box and the pectoralis muscle is indicated by the arrow in the transverse view. (d) The segmented breast is determined by the bounding box in the sagittal view.

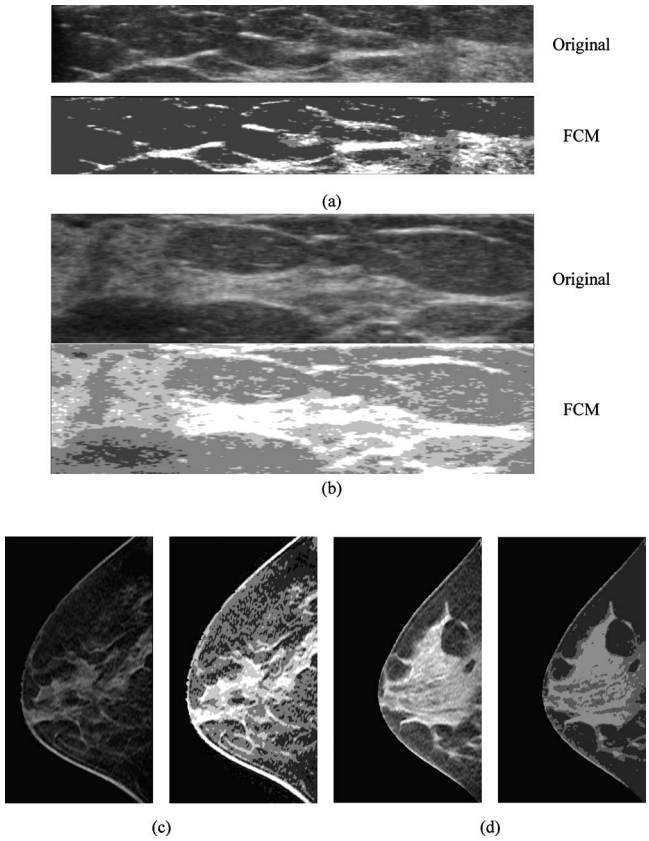

FIG. 6. (a) The original image and the result of FCM classifier on ABUS for a BIRADS mammographic density grade 2 case. (b) The original image and the result of FCM classifier on ABUS for a BIRADS mammographic density grade 3 case. The breast density is 30.28%. (c) The original image and the result of FCM classifier on MRI for the case in (a). The breast density on MRI is 18.66%. (d) The result of FCM classifier in 3-D breast MRI image for the case in (b). The breast density of 3-D breast MRI image is 35.68%.

the skin region might be considered as fibroglandular. Therefore, the skin needed to be removed and five pixels (1.95 mm) from the outer boundary of the breast region in each row were removed.

Upon complete segmentation of breast tissue, the FCM classifier was used for classifying the breast into fibroglandular and fatty tissue. The MRI percent breast density was then calculated. The MRI density was defined as

$$\text{percent density}_{\text{MRI}} = \frac{\text{fibroglandular volume}_{\text{MRI}}}{\text{total breast volume}_{\text{MRI}}}, \quad (2)$$

where the fibroglandular volume$_{\text{MRI}}$ is the volume of the fibroglandular tissue and the total breast volume$_{\text{MRI}}$ includes the volumes of the fibroglandular tissue and the fatty tissue.

II.E. Fuzzy C-mean classifier

After breast segmentation, the FCM classifier[18,21] was used to differentiate breast fibroglandular from fatty tissue and to calculate breast density. Breast anatomy within ABUS could be categorized into three structures: Hyperechoic, median echogenic, and hypoechoic.[26] Hyperechoic structures appear bright and include the skin, ribs, fasica, and fibroglandular tissue. Hypoechoic structures appear dark gray and include the mammary ducts and blood vessels. Medium echogenic structures appear median gray and include the fatty tissue, fibroglandular tissue, and muscle. The separation of the breast into three or four clusters, chosen by the operator, were assumed for ABUS and 3-D MRI images by the FCM classifier as shown in Fig. 6. With ABUS images for dense breasts, the variation of the gray intensity due to the speckle noise is large. Interoperator variation was evaluated within the experiment as a control. After determining the dense region and the breast region, the breast volume and the percent density could be calculated. For comparing the relationship between the ABUS images and the MRI images, the linear regression analysis was adopted. The linear regression analysis was performed by using SPSS for Windows (SPSS, Chicago, IL).

II.F. Comparison of breast densities measured from ABUS and MRI

We compared breast densities derived from ABUS images and MRI images as shown in Fig. 7. The correlation of the two modalities was represented by the fitted regression line defined as

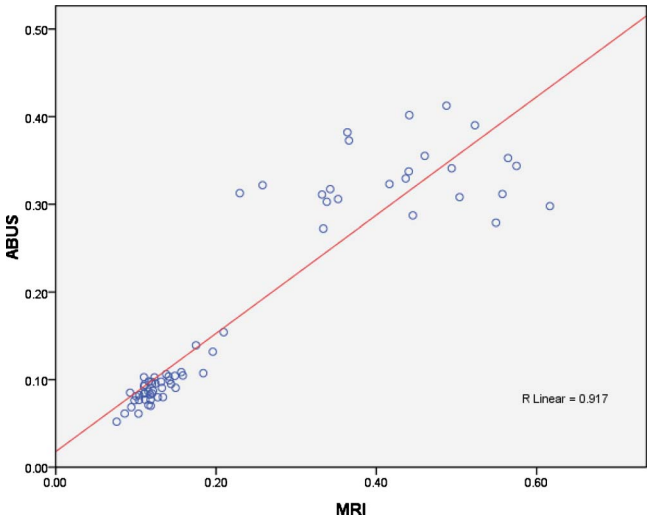

FIG. 7. The line regression of density of 3-D breast MRI and ABUS images and the correlation factor $R=0.917$.

$$Y_{\text{Modality}} = \text{Slope} \times X_{\text{Modality}} + \text{Const}, \quad (3)$$

where X_{Modality} is the density value of the X axis and Y_{Modality} is the density value of the Y axis. Slope and Const represent the regression line. The density correlation factor of two modalities is represented by R. The p value (<0.001), marker of significance level, was significant in our results.

II.G. Intraoperator and interoperator variation analyses

With 8 breasts randomly chosen from the 67, variations in both intraoperator and interoperator measurements, used when determining breast volume and density from the two imaging modalities, were analyzed. An operator analyzed these eight breasts three times. These three results' coefficients of variation (CVs) were compared to evaluate the consistency of one operator or intraoperator. Two additional operators also evaluated the same eight breasts. CVs of the measured breast volume and breast density were calculated from different operators and were compared to verify possible interoperator variation.

III. RESULTS

III.A. Intraoperator and interoperator variation analysis results

The calculated mean and standard variation of the breast volume density are listed in Table I. In the intraoperator analysis, the CV of volume and density was 4.21% (0.6%–6.84%) and 3.71% (0.81%–7.74%) for ABUS and 1.09% (0.21%–2.09%) and 0.80% (0.21%–2.61%) for MRI, respectively. Interoperator analysis yielded a CV of breast volume and density of 6.35% (0.42%–13.99%) and 6.34% (1.25%–9.94%) for ABUS images and 4.73% (1.25%–8.45%) and 3.05% (0.25%–12.35%) for MRI images, respectively. For case 6 of Table I, the ABUS cluster numbers of FCM se-

TABLE I. The intraoperator and interoperator variation analysis on ABUS and MRI images. The cluster number of FCM was selected by the operator. The first three were selected by operator 1 three times. The fourth and fifth values were the cluster numbers of FCM selected by operators 2 and 3.

		ABUS breast volume mean ± SD (cm^3)		ABUS breast density mean ± SD (%)	
Case No.	Cluster Number	Intraoperator	Interoperator	Intraoperator	Interoperator
1	3,3,3,3,3	381.48 ± 2.29 (0.60%)	372.81 ± 5.87 (1.57%)	7.17 ± 0.35 (4.90%)	7.78 ± 0.66 (8.53%)
2	3,3,3,3,3	500.48 ± 24.65 (4.93%)	535.13 ± 38.97 (7.28%)	7.19 ± 0.32 (4.51%)	7.83 ± 0.77 (9.82%)
3	3,3,3,3,3	405.64 ± 18.85 (4.65%)	425.76 ± 1.79 (0.42%)	12.82 ± 0.48 (3.72%)	13.03 ± 0.70 (5.40%)
4	3,3,3,3,3	437.09 ± 8.86 (2.03%)	415.48 ± 28.93 (6.96%)	16.47 ± 1.27 (7.74%)	15.63 ± 1.12 (7.18%)
5	4,4,4,4,4	318.26 ± 21.05 (6.61%)	328.64 ± 37.94 (11.54%)	30.50 ± 1.12 (3.66%)	29.54 ± 1.51 (5.12%)
6	4,4,4,4,3	352.53 ± 13.61 (3.86%)	361.04 ± 20.87 (5.78%)	28.65 ± 0.46 (1.62%)	28.14 ± 2.80 (9.94%)
7	3,3,3,3,3	378.74 ± 15.81 (4.18%)	383.33 ± 53.62 (13.99%)	10.55 ± 0.09 (0.81%)	10.69 ± 0.37 (3.45%)
8	3,3,3,3,3	383.49 ± 26.23 (6.84%)	362.54 ± 11.65 (3.21%)	12.41 ± 0.33 (2.69%)	11.96 ± 0.15 (1.25%)
	CV	4.21%	6.35%	3.71%	6.34%
		MRI breast volume mean ± SD (cm^3)		MRI breast density mean ± SD (%)	
Case No.	Cluster Number	Intraoperator	Interoperator	Intraoperator	Interoperator
1	4,4,4,4,4	661.68 ± 5.28 (0.80%)	635.21 ± 34.56 (5.44%)	10.30 ± 0.09 (0.86%)	10.51 ± 0.27 (2.54%)
2	4,4,4,4,4	675.68 ± 6.21 (0.92%)	709.41 ± 58.02 (8.18%)	13.05 ± 0.34 (2.61%)	12.67 ± 0.71 (5.59%)
3	4,4,4,4,4	619.02 ± 1.33 (0.21%)	636.97 ± 40.79 (6.40%)	19.15 ± 0.06 (0.30%)	19.20 ± 0.07 (0.35%)
4	4,4,4,4,4	624.43 ± 7.14 (1.14%)	629.37 ± 9.90 (1.57%)	19.48 ± 0.18 (0.92%)	19.44 ± 0.11 (0.58%)
5	3,3,3,4,3	538.94 ± 3.61 (0.67%)	535.58 ± 20.42 (3.81%)	37.34 ± 0.12 (0.31%)	34.81 ± 4.30 (12.35%)
6	3,3,3,3,3	491.08 ± 10.27 (2.09%)	494.04 ± 13.54 (2.74%)	41.16 ± 0.09 (0.21%)	41.14 ± 0.10 (0.25%)
7	4,4,4,4,4	756.68 ± 11.01 (1.45%)	797.55 ± 67.40 (8.45%)	20.04 ± 0.11 (0.56%)	20.27 ± 0.46 (2.27%)
8	4,4,4,4,4	711.16 ± 10.13 (1.42%)	714.11 ± 8.95 (1.25%)	20.82 ± 0.14 (0.65%)	20.80 ± 0.10 (0.47%)
	CV	1.09%	4.73%	0.80%	3.05%

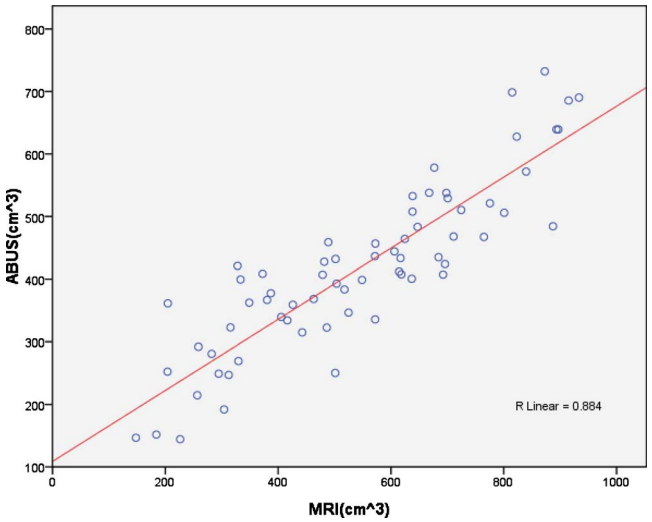

FIG. 8. The line regression of volume of 3-D breast MRI and ABUS images and the correlation factor $R=0.884$.

lected by operators were not the same resulting in variation (CV for percent density was 9.94%). The analyzed percent density was 28.92%, 30.46% and 25.03% by the three operators. For case 5 of Table I, the MRI cluster numbers of FCM selected by operators were also not the same, resulting in variation (CV=12.35%) in density calculations (29.41%, 31.11%, and 28.10%). These variations suggest that the percent density was affected by the cluster number selection.

III.B. Breast volume and percent breast density analysis from images of two modalities

Mean percent density and breast volume were, when using ABUS, $17.63 \pm 11.87\%$ and 418.30 ± 132.97 cm^3 and, when using MRI, $23.79 \pm 16.62\%$ and 544.90 ± 207.41 cm^3, respectively. The differences were not statistically significant ($p > 0.5$). In the breast density analysis, the correlation factor R was 0.917 and the slope of regression (Slope) was 0.675. The results showed that the breast density calculated from MRI image was larger than that of ABUS image.

The breast volumes derived from ABUS and MRI, both produced 3-D images, were compared in Fig. 8. The overall correlation factor R was 0.884 and the slope of the regression line was 0.568. The level of significance of slope p was less than 0.001. The results showed that the breast volume calculated from MRI image was larger than that of ABUS image.

III.C. The density and breast volume differences between left and right breasts

Differences in density and breast volume between the left and right breasts were analyzed for 27 patients in this experiment. The mean and standard deviation of volume differences between the breasts of a patient were 52.39 ± 36.05 cm^3 on ABUS and 73.71 ± 55.91 cm^3 on MRI. The mean and standard deviation of density difference between the left and right breasts of a patient were $1.96 \pm 2.43\%$ on ABUS and $2.13 \pm 2.03\%$ on MRI. Results demonstrate slight variation between the left and right breasts of a subject.

IV. DISCUSSION

With the increased use of ABUS for screening women with average to increased risk of breast cancer, the development of the algorithm to measure the breast density using multiple images will be important in investigating the relationship between breast density and breast cancer. Analysis of breast density based on ABUS is a new research area and, to the best of our knowledge, a comparison of the density analyzed from ABUS and MRI has not been performed. In this study, measurements of breast density and volume from 3-D ABUS and MRI images were found to be well correlated.

Using the similar anatomic landmark for the segmentation of the breast region, the measurement reproducibility analyses have shown that interoperator CVs on the two modalities were slightly larger than the intraoperator CVs. These results suggest that the proposed breast density analysis is reproducible. The average standard deviations of the breast volume and breast density on ABUS were, however, slightly larger than that on MRI. The reason for this discrepancy could be due to the fact that the boundary of the breast on MRI is obvious and could be defined more clearly than on ABUS.

From our experimental results, the quantitative values of percent density and breast volume measured by MRI were higher than those measured by ABUS. The reasons why the discrepancy of measured breast volume and breast density occurred between MRI and ABUS might include: (1) The patients were in the supine position during the ABUS scanning but were in the prone position for MRI, resulting in difference of the scanned breast regions; (2) two passes are used to scan the breast in ABUS and some regions might be overlapped or even missed; and (3) the percent density values measured from the two modalities are, in general, different due to the dense tissue, which might have different grey intensities. In our study, no ABUS cases with percent density in 16%–27% range were noted. It might be because that in this range there were only two corresponding MRI cases.

Bilateral breasts from the same subject may not be totally symmetrical. The intramodality left/right breast density measurement correlation in this study showed slight difference for the two imaging modalities. Meanwhile, in a study comparing MRI and mammography,[13] it was found that the intramodality left/right side correlation coefficients were 0.95 for MRI density and 0.84 for mammographic percent density, which were not significantly different. The mean absolute difference between sides was larger for the mammography (7.9%, 95%; CI=6.5–9.2) than for the MRI method (3.6%, 95%; CI=3.1–4.1, $p < 0.001$).

Two passes were used to scan the whole breast in ABUS resulting in a need to stitch the images of the two passes and remove the overlapping region before the breast analysis. Because the breasts of the patient were scanned in the supine position when the 3-D ABUS images were acquired, the

shape of the breast was deformed and extruded. The nipple was used as the landmark to cut the overlapping regions and the resulting coronal view was rechecked by an operator but error is still possible. Accurate segmentation of breast in ABUS also had its problems. The landmark for separating breast and nonbreast region in 3-D ABUS is not obvious. Since the pectoralis muscle may not be consistently well-recognized through all studied subjects, the use of the muscle as the anatomic landmark for breast segmentation may not be reliable. Either the fibroglandular tissue being omitted or the pectoralis muscle being included in the breast volume might happen. Due to inconsistent muscle curves unclearly defined by ABUS, utilization of the lowest horizontal plane in the C view to cut the nonbreast region manually was incapable of accurately separating breast tissue. Moreover, the muscle curves are not consistent in each slice, causing the need to manually cut each slice. In this study, the horizontal plane cutting line for all slices was used to maintain efficiency. In the future, an efficient method for cutting along inconsistent muscle curves for each slice should be found to improve the accuracy of density measurements.

The anatomic landmark used for segmenting the breast in 3-D ABUS and MRI images could result in the exclusion of some breast region. Among the few published MRI studies, the anatomic landmarks for MR-based breast segmentation methods were either not clearly specified[12,14,16,17,21,27] or used a simple boundary line drawn along the ventral surface of the pectoralis major muscle.[13,15,28] A recently published paper by Nie *et al.*[18] described using V-shaped landmarks of each individual woman to determine the lateral posterior boundary of the breast to separate the breast from body fat. Nie's method, however, requires images with a large field of view that include the whole chest cavity containing the thoracic spinous process. The present development of such MR-based breast density measurement techniques is still in its infancy and it is not clear yet as to which landmark can provide more consistent segmentation results of breast volume.

Possible errors could also be due to the FCM utilized in segmenting fibroglandular tissue from breast region. Klifa *et al.*[27] compared the segmented results of intrauser and interuser for manual, global threshold, and FCM. The results showed that the FCM had less user variation than two other methods. However, while FCM can automatically select cluster means to separate the image into clusters, the determining of a suitable number of clusters, also important to have a good analysis result, is flexible. Despite ABUS breast anatomy's possible categorization into three structures, three clusters might not be suitable for all cases. This is why operators were allowed to choose among three or four clusters. In the study of Nie *et al.*,[18] three or four clusters were used to segment fibroglandular tissue in MRI. In the results of the intraoperator and interoperator variations, however, different clusters numbers could have caused the variations in calculated breast density. For the cases of Table I with different number of clusters in ABUS and MRI images, the interoperator variations were larger than most of the other cases using the same number of clusters. Furthermore, the variation (12.35%) in MRI images was higher than that (9.94%) in ABUS images.

V. CONCLUSION

In this study, we compared the measurement of breast density on ABUS and MRI. In our experiments, breast volume and percent breast density measured by 3-D ABUS and MRI images were well correlated. Our results indicate that both ABUS and MRI densities could provide useful breast density information to physician. Further improvement for the segmentation of the breast region and the fibroglandular tissue is needed to improve the density analysis with ABUS.

ACKNOWLEDGMENTS

This work was supported by the National Science Council, Taiwan, Republic of China, under Grant No. NSC 96-2221-E-002-268-MY3 and supported in part by NIH/NCI Grant No. R03 CA136071.

[a]Authors to whom correspondence should be addressed.
[b]Electronic mail: jeonhc@uci.edu
[c]Electronic mail: rfchang@csie.ntu.edu.tw

[1]H. Johansson, S. Gandini, B. Bonanni, F. Mariette, A. Guerrieri-Gonzaga, D. Serrano, E. Cassano, F. Ramazzotto, L. Baglietto, M. T. Sandri, and A. Decensi, "Relationships between circulating hormone levels, mammographic percent density and breast cancer risk factors in postmenopausal women," Breast Cancer Res. Treat. **108**, 57–67 (2008).
[2]N. F. Boyd, G. S. Dite, J. Stone, A. Gunasekara, D. R. English, M. R. McCredie, G. G. Giles, D. Tritchler, A. Chiarelli, M. J. Yaffe, and J. L. Hopper, "Heritability of mammographic density, a risk factor for breast cancer," N. Engl. J. Med. **347**, 886–894 (2002).
[3]E. Ziv, J. Shepherd, R. Smith-Bindman, and K. Kerlikowske, "Mammographic breast density and family history of breast cancer," J. Natl. Cancer Inst. **95**, 556–558 (2003).
[4]J. Stone, G. S. Dite, A. Gunasekara, D. R. English, M. R. McCredie, G. G. Giles, J. N. Cawson, R. A. Hegele, A. M. Chiarelli, M. J. Yaffe, N. F. Boyd, and J. L. Hopper, "The heritability of mammographically dense and nondense breast tissue," Cancer Epidemiol. Biomarkers Prev. **15**, 612–617 (2006).
[5]M. L. Irwin, E. J. Aiello, A. McTiernan, L. Bernstein, F. D. Gilliland, R. N. Baumgartner, K. B. Baumgartner, and R. Ballard-Barbash, "Physical activity, body mass index, and mammographic density in postmenopausal breast cancer survivors," J. Clin. Oncol. **25**, 1061–1066 (2007).
[6]J. Brisson, S. Berube, C. Diorio, M. Sinotte, M. Pollak, and B. Masse, "Synchronized seasonal variations of mammographic breast density and plasma 25-hydroxy vitamin d," Cancer Epidemiol. Biomarkers Prev. **16**, 929–933 (2007).
[7]N. F. Boyd, H. Guo, L. J. Martin, L. Sun, J. Stone, E. Fishell, R. A. Jong, G. Hislop, A. Chiarelli, S. Minkin, and M. J. Yaffe, "Mammographic density and the risk and detection of breast cancer," N. Engl. J. Med. **356**, 227–236 (2007).
[8]V. A. McCormack and I. dos Santos Silva, "Breast density and parenchymal patterns as markers of breast cancer risk: A meta-analysis," Cancer Epidemiol. Biomarkers Prev. **15**, 1159–1169 (2006).
[9]C. M. Vachon, V. S. Pankratz, C. G. Scott, S. D. Maloney, K. Ghosh, K. R. Brandt, T. Milanese, M. J. Carston, and T. A. Sellers, "Longitudinal trends in mammographic percent density and breast cancer risk," Cancer Epidemiol. Biomarkers Prev. **16**, 921–928 (2007).
[10]J. A. Harvey and V. E. Bovbjerg, "Quantitative assessment of mammographic breast density: Relationship with breast cancer risk," Radiology **230**, 29–41 (2004).
[11]D. B. Kopans, "Basic physics and doubts about relationship between mammographically determined tissue density and breast cancer risk," Radiology **246**, 348–353 (2008).
[12]J. Eng-Wong, J. Orzano-Birgani, C. K. Chow, D. Venzon, J. Yao, C. E. Galbo, J. A. Zujewski, and S. Prindiville, "Effect of raloxifene on mam-

mographic density and breast magnetic resonance imaging in premenopausal women at increased risk for breast cancer," Cancer Epidemiol. Biomarkers Prev. **17**, 1696–1701 (2008).
[13]M. Khazen, R. M. Warren, C. R. Boggis, E. C. Bryant, S. Reed, I. Warsi, L. J. Pointon, G. E. Kwan-Lim, D. Thompson, R. Eeles, D. Easton, D. G. Evans, and M. O. Leach, "A pilot study of compositional analysis of the breast and estimation of breast mammographic density using three-dimensional T1-weighted magnetic resonance imaging," Cancer Epidemiol. Biomarkers Prev. **17**, 2268–2274 (2008).
[14]J. Wei, H. P. Chan, M. A. Helvie, M. A. Roubidoux, B. Sahiner, L. M. Hadjiiski, C. Zhou, S. Paquerault, T. Chenevert, and M. M. Goodsitt, "Correlation between mammographic density and volumetric fibroglandular tissue estimated on breast MR images," Med. Phys. **31**, 933–942 (2004).
[15]S. van Engeland, P. R. Snoeren, H. Huisman, C. Boetes, and N. Karssemeijer, "Volumetric breast density estimation from full-field digital mammograms," IEEE Trans. Med. Imaging **25**, 273–282 (2006).
[16]N. A. Lee, H. Rusinek, J. Weinreb, R. Chandra, H. Toth, C. Singer, and G. Newstead, "Fatty and fibroglandular tissue volumes in the breasts of women 20–83 years old: Comparison of x-ray mammography and computer-assisted MR imaging," AJR, Am. J. Roentgenol. **168**, 501–506 (1997).
[17]J. Yao, J. A. Zujewski, J. Orzano, S. Prindiville, and C. Chow, "Classification and calculation of breast fibroglandular tissue volume on SPGR fat suppressed MRI," in *SPIE International Symposium Medical Imaging 2005: Image Processing*, edited by J. M. Fitzpatrick and J. M. Reinhardt (SPIE, Bellingham, 2005), pp. 1942–1949.
[18]K. Nie, J. H. Chen, S. Chan, M. K. Chau, H. J. Yu, S. Bahri, T. Tseng, O. Nalcioglu, and M. Y. Su, "Development of a quantitative method for analysis of breast density based on three-dimensional breast MRI," Med. Phys. **35**, 5253–5262 (2008).
[19]J. A. Harvey, R. E. Hendrick, J. M. Coll, B. T. Nicholson, B. T. Burkholder, and M. A. Cohen, "Breast MR imaging artifacts: How to recognize and fix them," Radiographics **27**, S131–S145 (2007).
[20]C. K. Glide-Hurst, N. Duric, and P. Littrup, "Volumetric breast density evaluation from ultrasound tomography images," Med. Phys. **35**, 3988–3997 (2008).
[21]C. Klifa, J. Carballido-Gamio, L. Wilmes, A. Laprie, J. Shepherd, J. Gibbs, B. Fan, S. Noworolski, and N. Hylton, "Magnetic resonance imaging for secondary assessment of breast density in a high-risk cohort," Magn. Reson. Imaging **28**, 8–15 (2010).
[22]J.-H. Chen, C.-S. Huang, K.-C. C. Chien, E. Takada, W. K. Moon, J. H. K. Wu, N. Cho, Y.-F. Wang, and R.-F. Chang, "Breast density analysis for whole breast ultrasound images," Med. Phys. **36**, 4933–4943 (2009).
[23]K. M. Kelly, J. Dean, W. S. Comulada, and S. J. Lee, "Breast cancer detection using automated whole breast ultrasound and mammography in radiographically dense breasts," Eur. Radiol. **20**, 734–742 (2010).
[24]R.-F. Chang, K.-C. Chang-Chien, H.-J. Chen, D.-R. Chen, E. Takada, and W. Kyung Moon, "Whole breast computer-aided screening using freehand ultrasound," International Congress Series **1281**, 1075–1080 (2005).
[25]Q. L. Sun, J. A. Hossack, J. S. Tang, and S. T. Acton, "Speckle reducing anisotropic diffusion for 3D ultrasound images," Comput. Med. Imaging Graph. **28**, 461–470 (2004).
[26]L. Watson, "The role of ultrasound in breast imaging," Radiol. Technol. **71**, 441–459 (2000).
[27]C. Klifa, J. Carballido-Gamio, L. Wilmes, A. Laprie, C. Lobo, E. DeMicco, M. Watkins, J. Shepherd, J. Gibbs, and N. Hylton, "Quantification of breast tissue index from MR data using fuzzy clustering," in Engineering in Medicine and Biology Society, 2004, IEMBS '04: Proceedings of the 26th Annual International Conference of the IEEE, Vol. 1, pp. 1667–1670, 2004 (unpublished).
[28]D. Thompson, M. Leach, G. Kwan-Lim, S. Gayther, S. Ramus, I. Warsi, F. Lennard, M. Khazen, E. Bryant, S. Reed, C. Boggis, D. G. Evans, R. Eeles, D. Easton, and R. Warren, "Assessing the usefulness of a novel MRI-based breast density estimation algorithm in a cohort of women at high genetic risk of breast cancer: The UK MARIBS study," Breast Cancer Res. Treat. **11**, R80 (2009).